

Fast, Reusable, Cell Uniformly Distributed Membrane Filtration Device for Separation of Circulating Tumor Cells

Jintao Han, Chunyang Lu, Mengzhu Shen, Xiaoyi Sun, Xiaodong Mo, and Gen Yang*

Cite This: *ACS Omega* 2022, 7, 20761–20767

Read Online

ACCESS |



Metrics & More

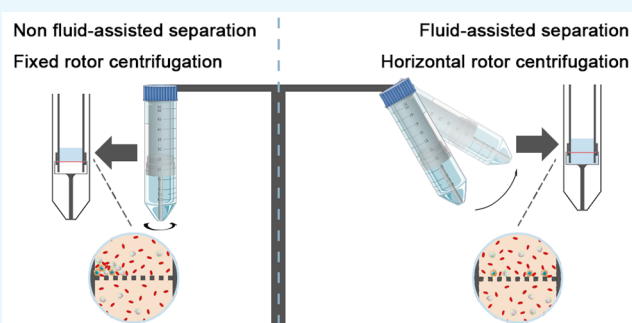


Article Recommendations



Supporting Information

ABSTRACT: Isolation of circulating tumor cells (CTCs) is of great significance for the diagnosis, prognosis, and treatment of metastatic cancer. Among CTC capture methods independent of antibodies, membrane filtration-based methods have the advantages of simplicity, rapidity, and high throughput but usually have problems such as clogging, high pressure drop, and impaired cell viability. In this study, we designed and tested a reusable device that used horizontal rotor and fluid-assisted separation to capture CTCs by centrifugal membrane filtration, achieving simple, fast, highly efficient, and viable cell capture on traditional centrifuge. The average capture efficiency was 95.8% for different types of cancer cells with >90% survival, and the removal of white blood cells can reach 99.72% under four times cleaning of the membrane after filtration. A further clinic demo was performed using the device to detect residual leukemic cells in patients; the results showed a 10-fold enrichment of the leukemic cells in peripheral blood samples. Taken together, the simple, robust, and efficient CTC capture device may have the potential for clinic routine detection and analysis of circulating tumor cells.



1. INTRODUCTION

Cancer metastases cause about 90% of cancer-related deaths.¹ Circulating tumor cells (CTCs) are cancer cells that shed from primary tumor sites to blood or lymph vessels and have the potential to induce metastasis in distant tissues or organs through the blood circulatory system.^{2,3} In many cancers, the number of CTCs correlates with the progression-free survival (PFS) and overall survival (OS) of patients;^{4,5} hence, the diagnostic and prognostic prediction by CTCs is prospective in cancer control of patients.^{6,7} CTCs are recognized as a biomarker for tumor progress and therapeutic response,⁸ the surveillance of CTCs is of great significance for clinical applications, such as early metastatic detection and individual treatment plan choice,^{9,10} and CTCs from patients can also be used for drug resistance tests and therapeutic targets' searches.¹¹

The first step for CTC analysis is the capture of CTCs, and it is crucial to obtain intact and viable CTCs for various applications. However, this has always been challenging since CTCs are rare and fragile in peripheral blood.¹² Nowadays, methods using the biological or physical properties of CTCs and methods combined to detect or capture CTCs are gradually emerging;¹³ however, there is still a long way to go to reach extensive clinical routine use. The immunocapture methods show good specificity but deeply rely on the expression level of cell surface biomarkers.¹⁴ The heterogeneity and epithelial–mesenchymal transition (EMT) of cancer cells are sure to result in loss of detected CTCs in affinity-based methods,¹⁵ and the attachment of target cells to the artificial surface will definitely

affect the viability of cells.¹⁶ Besides, antibody-based methods are usually expensive and time-consuming with the biochemical marker reagents usage and surface modification process.¹⁷

The CTC enrichment methods based on physical properties utilize the size, shape, density, or deformability difference between CTCs and blood cells, showing advantages for rapid and label-free analysis.¹⁸ Microchip-based streamline or filtration methods can reach high flow rate but usually are sensitive to it, and these methods often need special requirements or have poor robustness.¹⁹ On the other hand, the micropore filtration methods are simple, low cost, and easy to operate and can reach high throughput and recovery.^{20,21} However, there are usually the problems of clogging, high pressure drop, and cell viability damage.²² In order to improve the performance of membrane filtration, many researches attempted to design a new filter structure or filtration device, such as a separable bilayer (SB) microfiltration device or fabric filter device.^{23,24} Fluid-assisted separation technology (FAST) is a method inspired by antifouling membranes with liquid-filled pores in nature, which has the advantage of low pressure drops in

Received: February 25, 2022

Accepted: May 6, 2022

Published: June 8, 2022



filtration processes and may have prospects in the application of centrifugal filtration.²⁵

With regard to the cancer cell identification, a combination of antibodies is usually used for different cells; however, the immunobinding process is rather complex and time-consuming.²⁶ As widely used in clinical diagnosis, especially in the detection of hematologic disorders, morphological examination by using Wright–Giemsa staining and microscope investigation can provide the detailed structure of cells and has the advantage of simpleness, quickness, and good accuracy.^{27,28}

Due to the shortness and limited application of different CTC capture methods, there is still urgent need for simple, high-throughput, highly efficient and viable CTC capture methods for large volume clinical samples. Here we design a device that realizes self-adapting to a uniform cell distribution on a membrane by horizontal rotor and fluid-assisted separation. Using the device, we can achieve label-free CTC capture with high throughput, high capture efficiency, and high viability, and combined with morphological examination, the separation and identification of cancer cells can be realized in the meantime during filtration. For clinical applications such as point-of-care testing of patient blood samples, the device may be used for routine cancer detection and analysis since it is simple, rapid, robust, and reusable.

2. RESULTS

2.1. Design Principles of the Filtration Device. As shown in Figures 1a, 2d, and S1, the filtration device was designed for the realization of fluid-assisted CTC separation in a

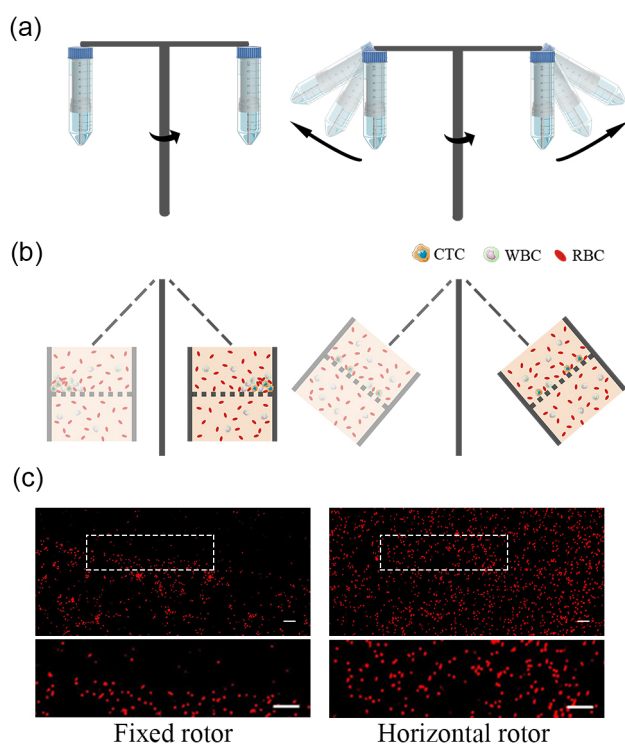


Figure 1. Operating principles of the device. (a) Schematic illustration of the centrifugal process. (b) Schematic illustration of the performance of blood cells on the membrane during centrifugation. (c) Distribution of red fluorescent protein (RFP)-stained HeLa cells on the membrane during centrifugation. The lower image is a zoomed picture of the upper image in the dotted box. (Scale bar: 100 μm .)

traditional centrifuge with the device assembled in a 50 mL centrifuge tube, and the horizontal rotor was used to avoid uneven cell stress during centrifugation; thus, the cells distributed uniformly on the membrane and simple, rapid, highly efficient CTC capture was achieved (Figure 1b).

In order to compare the cells' performance on the membrane when centrifuged in a different way, HeLa cells stained red were filtrated in a fixed or horizontal rotor and imaged with a low-magnification microscope. The results are shown in Figure 1c: the distribution of cells using the fixed rotor was uneven, and cells were found at the edge of the membrane, while cells using the horizontal rotor were uniformly distributed on the membrane, avoiding cell capture efficiency reduction and cell viability damage caused by clogging.

2.2. Design Parameters of the Filtration Device. The design parameters of the device are shown in Figure 2a, and it consisted of four parts (Figure 2b and c). The top cylindrical chamber was used for sample injection, the bottom tank was a liquid reservoir, and the middle component comprised of upper and lower parts was used to place the membrane. There were grooves or notches in the two parts, which were used for the flow of the liquid to the 50 mL tube (Figure 2d). The sample volume injected to the device can be as large as 15 mL, and the centrifugation process was usually finished in 1 min. Therefore, rapid, high-throughput liquid sample analysis can be achieved.

2.3. Characterization of the Filtration Membrane Used in the Device. The characterization of the filtration membrane by SEM is demonstrated in Figure S2a, and the size distribution of the membrane pore is shown in Figure S2b, with an average pore size of $6.881 \pm 0.592 \mu\text{m}$ ($n = 100$) and porosity of 3.3%. Besides, membranes with different pore sizes or porosities can also be assembled in the device for CTC capture. The images of the membrane before and after filtration of the blood sample are shown in Figure S2c, demonstrating the device can be used for simple and rapid liquid sample analysis.

2.4. Validation of the Device Using Cancer Cells in Culture Medium or Spiked in Blood. The capture efficiency of cancer cells in culture medium or spiked in blood was measured using different cell densities and cell lines. RFP-labeled cancer cells were added in the device for centrifugal filtration, and the cells on the membrane and flowing out from the device were counted. The results of capture efficiency are shown in Figure S3a and b for culture medium sample and Figure 3a and b for the blood sample. In order to simulate the clinical CTC concentration in patient blood, the densities of the cancer cells were set at the range 1–600 cells/mL. The average capture efficiency showed good linearity and was 96.2% and 95.1% in the culture medium and blood, respectively. The capture efficiencies of four cell lines, including cervical cancer HeLa cells, colon cancer SW620 cells, breast cancer MDA-MB-231 cells, and lung cancer NCI-H226 cells, were detected, and the average efficiencies in blood were 94.6%, 97.8%, 95.7%, and 94.9%, respectively. For the cancer cells in the culture medium or spiked in blood, the average capture efficiency for the four cell lines was $95.4 \pm 0.8\%$ and $95.8 \pm 1.4\%$, indicating the device can be used to capture different types of cancer cells with different sizes and deformabilities.

Purity was important for CTC detection and analysis, so rapid and efficient WBCs' removal in blood samples was significant. The fluorescent images of cancer cells (red) and WBCs (blue) on the membrane and flow out of the device after filtration are shown in Figures 3c and S3c, respectively. It was evident that

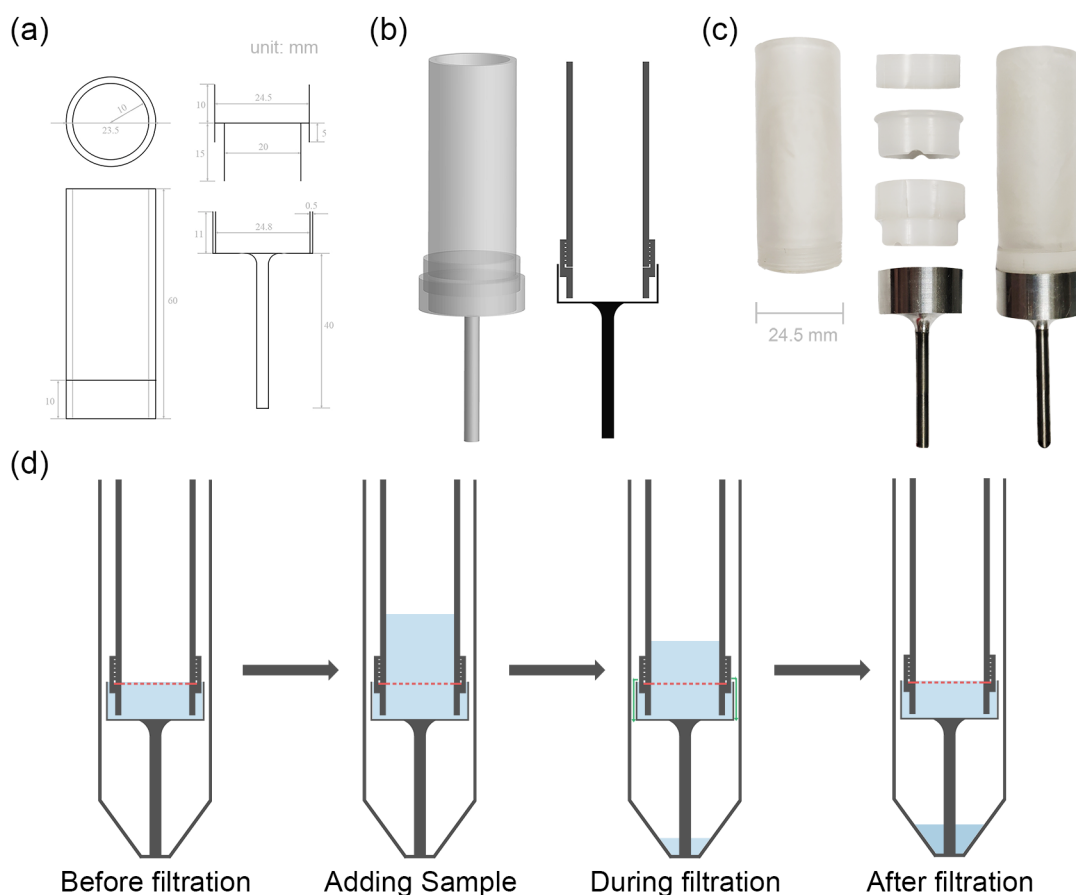


Figure 2. Design of the filtration device. (a) Design parameter of the device. (b) Schematic illustration of the device. (c) Picture of the device. Photograph courtesy of Jintao Han. Copyright 2020. (d) Schematic illustration of the liquid flow in the device during the filtration process.

most of the cancer cells were collected on the membrane while the majority of WBCs flowed out of the membrane.

The wash times of the membrane using PBS after filtration affected not only the removal of WBCs but also the detection of CTCs; hence, the depletion ratio of WBCs and the capture efficiency of cancer cells were calculated under different washing times. As shown in Figure 3d, for washing 0–4 times, the log depletion ratio of WBCs was 1.91 ± 0.21 , 1.99 ± 0.18 , 2.18 ± 0.13 , 2.34 ± 0.23 , and 2.55 ± 0.15 . With WBCs' removal proportion increased from 98.78% to 99.72%, the capture efficiency of cancer cells was 94.6%, 94.4%, 96.0%, 93.1%, and 91.2% at 0–4 washing times, indicating the validity of the device used for CTC capture.

In order to further compare the performance of CTC detection at different centrifugal modes, the capture efficiency of cancer cells and the depletion ratio of WBCs were measured using a horizontal rotor or fixed rotator and FAST or non-FAST centrifugation. From the results shown in Figure S3d, we find that when capturing the cancer cells spiked in blood using the horizontal rotor and FAST centrifugation, both the capture efficiency and depletion ratio showed promotion compared with the fixed rotator and non-FAST centrifugation.

2.5. Viability and Growth Verification of Cancer Cells after Separation. Since survival of captured cells is also vital for further cell analysis and testing, the viability and growth of cancer cells after centrifugal filtration were detected. As shown in Figure 4a–b, green fluorescence demonstrated good viability of captured cancer cells and the survival rate was 90.2% and 94.4%

at the first and tenth day, respectively. The difference of cell viability between experiment and control group was not significant, indicating that the filtration process had little damage on cancer cells.

Figure 4c–d showed the images of captured cells at 1–5 day after filtration and corresponding growth curve. Cells grew well in both experiment and control group, the cell counts had no significant difference and the curve both fitted growth curve model well.

2.6. Isolation of Residual Leukemic Cells from Patients Received Treatment. Detected immature cells in peripheral blood indicated emergence or relapse of the blood disease. We analyzed the peripheral blood of acute leukemia patients who had received treatment, and the residual leukemic cells were enriched by the device and the staining process was finished during filtration. As demonstrated in Figure 5a and b, the cells stained by Wright–Giemsa clearly showed the size and structure of the cell and its nuclei, and the leukemic cell percentage of patients by counting 100–800 cells in three parallel groups is shown in Figure 5c. For patient-1 and patient-3, whose cancer cells were undetectable in peripheral blood, the leukemic cell percentage after enrichment was 2.3% and 13.9% respectively, and for patient-2 the leukemic cell percentage increased from 1% to 10.7%, indicating 10-fold improvement for cancer cell detection.

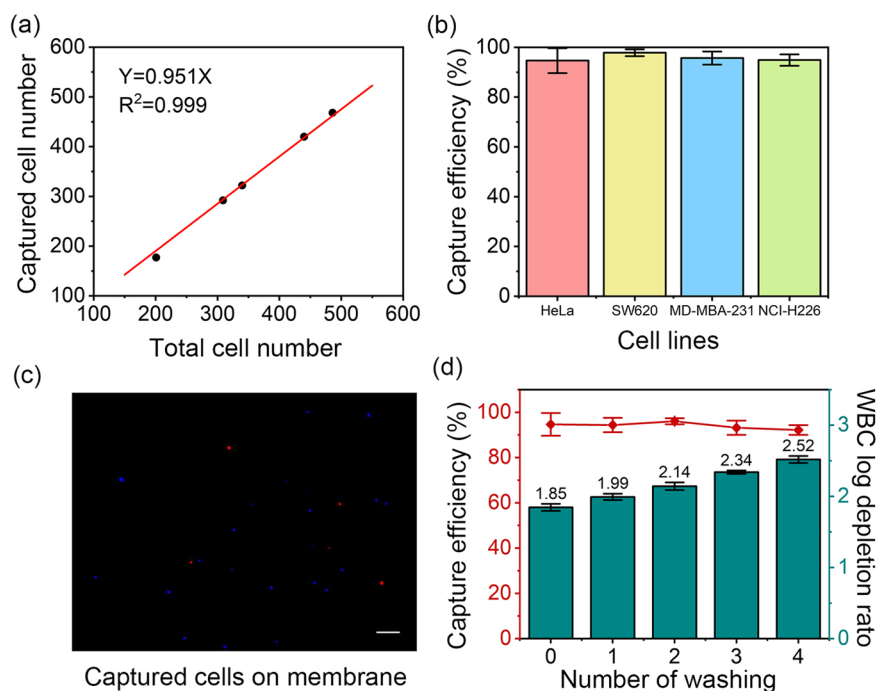


Figure 3. Device validation using cells spiked in blood. (a) Capture efficiency for different cell densities using HeLa cells spiked in blood. Regression analysis is shown. (b) Capture efficiency for cervical cancer HeLa cells, colon cancer SW620 cells, breast cancer MDA-MB-231 cells, and lung cancer H226 cells spiked in blood ($n = 3$). (c) Merged view of cancer cells (red) and white blood cells (WBCs) (blue) on the membrane after filtration of blood spiking sample. (Scale bar: $100 \mu\text{m}$.) (d) Capture efficiency and WBC depletion ratio of HeLa cells spiked in blood under different PBS wash times of the membrane after centrifugation ($n = 3$).

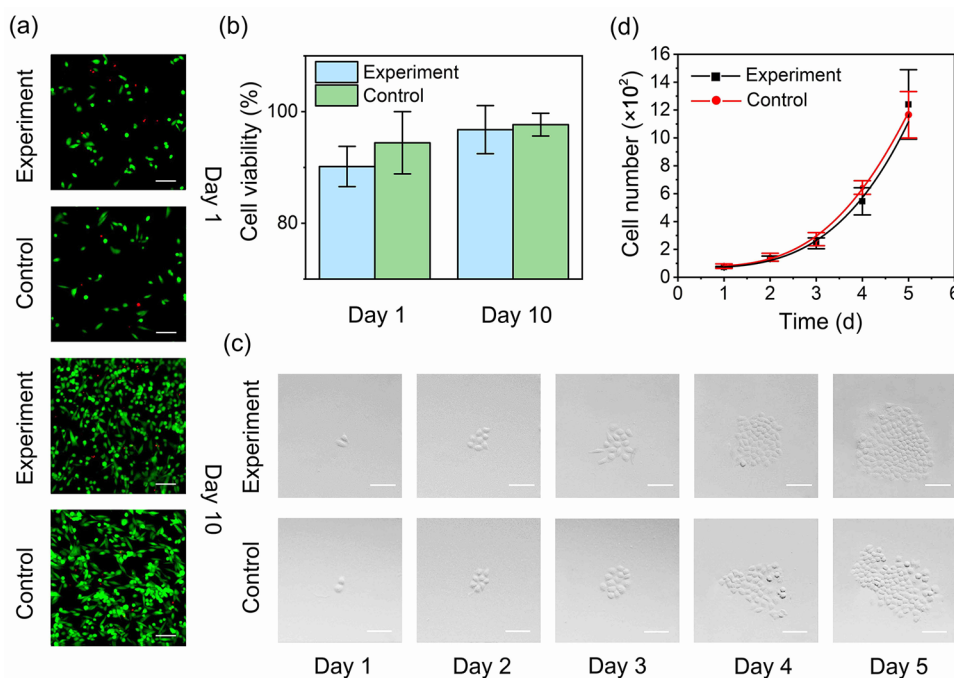


Figure 4. Cancer cells collected by the device. (a) Images of the cell viability of the control and the collected cells at days 1 and 10. (Scale bar: $100 \mu\text{m}$.) (b) Statistics of the cell survival rate of the control and the collected cells ($n = 3$). (c) Images of cell growth of the control and the collected cells over time. (Scale bar: $100 \mu\text{m}$.) (d) Growth curves of the control and the collected cells ($n = 3$).

3. DISCUSSIONS AND CONCLUSIONS

Although many researches revealed the potential value of CTCs in cancer diagnosis, prognosis, and treatment, the application of CTC detection in the clinical environment still faces major challenges. Large sample volumes and multiple blood draws may

be requirements for CTC analysis in the future and may provide more information about patients. Membrane filtration and other size-based methods used for CTC capture have shown great prospects in application with the advantages of simpleness, rapidness, and high throughput. However, in the face of complex

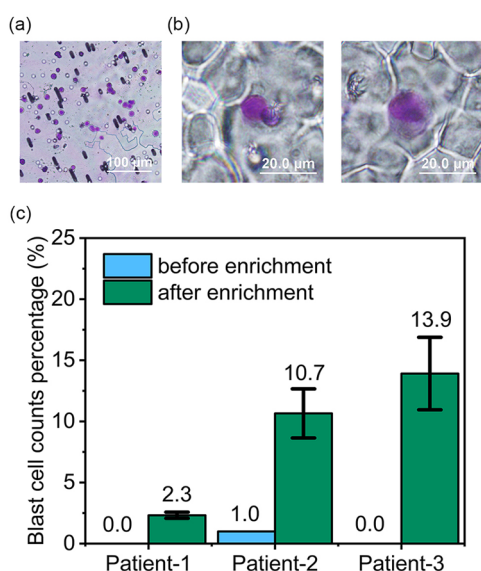


Figure 5. Leukemic cell detection of patients by the device. (a) Image of the membrane after Wright–Giemsa staining. (Scale bar: 100 μm .) (b) Representative images of blood cells in patients. (Scale bar: 20 μm .) (c) Percentage of the leukemic cells in the peripheral blood of patients before and after enrichment.

liquid samples and high standard requirements, more preclinical tests and large-scale, multicenter clinical trials are needed.

In this study, we designed and tested a membrane filtration device using a horizontal rotor and fluid-assisted separation to capture cancer cells in blood. The device can be assembled into a 50 mL centrifuge tube and was able to realize simple, fast (1 min), cheap (reusable), efficient ($\sim 95\%$), and viable ($>90\%$) cell capture on a conventional centrifuge, indicating the potential of the device used for clinic routine detection and analysis of circulating tumor cells. Besides, the ability of the filtration device to analyze and process large volumes of liquid with high efficiency and high throughput was sure to have important clinical significance. Furthermore, different types of filtration membranes can be placed in the device and membranes with higher porosity may be used to achieve more effective WBC removal and more high-throughput liquid sample analysis.

The enrichment of cancer cells by centrifugal filtration was combined with morphological examination of cells on the membrane by Wright–Giemsa staining in our study, realizing both cell separation and identification at the same time. For the detection of residual leukemic cells in the peripheral blood of patients post treatment, the device realized 10-fold enrichment of the cancer cells, making close surveillance of patients possible in routine. With regard to the clinical blood samples of different patients, the critical size for separating leukemic cells and normal WBCs needs to be adjusted according to the unique size distribution of different patients' blood cells for better device performance. Besides, more blood sample analysis of different types of leukemia is necessary to explore the application potential of the method, and for further application, cells collected after enrichment can be used to investigate drug resistance or search for potential therapeutic targets.

4. MATERIALS AND METHODS

4.1. Device Fabrication. The device is fabricated according to the design from metal aluminum (Al) and polyamide (PA) using Turning technology. The device was assembled with a

membrane and fit into 50 mL centrifuge tubes (Coring) for cell separation experiments.

4.2. Cell Culture and Blood Collection. HeLa, SW620, and MDA-MB-231 cells were cultured in DMEM high-glucose medium (HyClone), and NCI-H226 cells were cultured in RPMI 1640 medium (HyClone). The cell culture media were all supplemented with 10% fetal bovine serum (FBS, Bai Ling Biotechnology) and 1% penicillin–streptomycin (P/S) (HyClone). All of the cells were cultured in the incubator at the conditions of 37 $^{\circ}\text{C}$ and 5% CO_2 . The rabbit blood was used for preclinical cancer cell spiking experiments since the components in rabbit blood are similar to human blood and it is convenient to obtain animal blood.²⁹ The rabbit blood was collected in lithium heparin tubes (BD Vacutainer), and 10 mg/mL heparin sodium solution (Yuanye) was added to avoid coagulation.

4.3. Cell Isolation Process. For the formation of fluid-assisted separation and prevention of cell adhesion, a device assembled with a membrane was added 3 mL of 1% BSA (bovine serum albumin, Amresco), centrifuged at 300 rpm for 1 min, and then left at room temperature for 30 min. As shown in Figure S1b, a 1 mL cell suspension of spiked blood was added to the device and centrifuged at 300 rpm for 1 min with or without PBS wash. The device was then disassembled, and the membrane and liquid at the bottom of the 50 mL centrifuge tube were collected for cell imaging.

4.4. Viability and Growth Curve of Cells before and after Filtration. The Calcein-AM/PI staining kit (BestBio) was used to assay the viability of isolated cancer cells. Live cells and dead cells showed green and red fluorescence, respectively. For the verification of cell proliferation ability before and after filtration, the isolated cancer cells were cultured at 37 $^{\circ}\text{C}$ in a humidified incubator (5% CO_2). The number of cells was counted at days 1, 2, 3, 4, and 5, and the growth curve was plotted and fit by a growth formula.

4.5. Leukemic Cells' Isolation from Patients' Peripheral Blood. The peripheral blood of leukemia patients was obtained from Peking University People's Hospital. All participants gave written informed consent in accordance with the Declaration of Helsinki, and approval was given by the Peking University People's Hospital Institutional Review Board (2021PHB125-001). ACK lysing buffer (Gibco) was added to blood at 4 $^{\circ}\text{C}$ to remove red blood cells, and the cell solution was transferred to a freezing tube for storage. When performing experiments, the diluted patient sample was stained by Wright–Giemsa stain and filtrated by the device with an Isopore Polycarb membrane. The cells on the membrane were imaged by a microscope under a bright field.

■ ASSOCIATED CONTENT

SI Supporting Information

The Supporting Information is available free of charge at <https://pubs.acs.org/doi/10.1021/acsomega.2c01153>.

Supplementary figures for device operating details, filtration membrane characterization, and additional device validation; materials and methods for membrane characterization, isolation of cancer cells, the cell distribution test, and Wright–Giemsa staining of cells (PDF)

AUTHOR INFORMATION

Corresponding Author

Gen Yang – State Key Laboratory of Nuclear Physics and Technology, School of Physics, Peking University, Beijing 100871, China; Wenzhou Institute, University of Chinese Academy of Sciences, Wenzhou 352001, China; Email: gen.yang@pku.edu.cn

Authors

Jintao Han – State Key Laboratory of Nuclear Physics and Technology, School of Physics, Peking University, Beijing 100871, China; orcid.org/0000-0002-0731-7006

Chunyang Lu – State Key Laboratory of Nuclear Physics and Technology, School of Physics, Peking University, Beijing 100871, China

Mengzhu Shen – Beijing Key Laboratory of Hematopoietic Stem Cell Transplantation, Peking University Institute of Hematology, Peking University People's Hospital, Beijing 100044, China

Xiaoyi Sun – State Key Laboratory of Nuclear Physics and Technology, School of Physics, Peking University, Beijing 100871, China

Xiaodong Mo – Beijing Key Laboratory of Hematopoietic Stem Cell Transplantation, Peking University Institute of Hematology, Peking University People's Hospital, Beijing 100044, China

Complete contact information is available at:

<https://pubs.acs.org/10.1021/acsomega.2c01153>

Notes

The authors declare no competing financial interest.

ACKNOWLEDGMENTS

This research was supported by the National Natural Science Foundation of China (11875079) and the State Key Laboratory of Nuclear Physics and Technology, PKU, under Grant No. NPT2020KFY19.

REFERENCES

- (1) Chaffer, C. L.; Weinberg, R. A. A Perspective on Cancer Cell Metastasis. *Science* **2011**, *331* (6024), 1559–1564.
- (2) Cheung, K. J.; Ewald, A. J. A collective route to metastasis: Seeding by tumor cell clusters. *Science* **2016**, *352* (6282), 167–169.
- (3) Hanahan, D.; Weinberg, R. A. The hallmarks of cancer. *Cell* **2000**, *100* (1), 57–70.
- (4) Janni, W. J.; Rack, B.; Terstappen, L. W. M. M.; Pierga, J. Y.; Taran, F. A.; Fehm, T.; Hall, C.; de Groot, M. R.; Bidard, F. C.; Friedl, T. W. P.; et al. Pooled Analysis of the Prognostic Relevance of Circulating Tumor Cells in Primary Breast Cancer. *Clin. Cancer Res.* **2016**, *22* (10), 2583–2593.
- (5) Shishido, S. N.; Carlsson, A.; Nieva, J.; Bethel, K.; Hicks, J. B.; Bazhenova, L.; Kuhn, P. Circulating tumor cells as a response monitor in stage IV non-small cell lung cancer. *J. Transl. Med.* **2019**, *17* (1), DOI: [10.1186/s12967-019-2035-8](https://doi.org/10.1186/s12967-019-2035-8).
- (6) Van Dalum, G.; Stam, G. J.; Scholten, L. F. A.; Mastboom, W. J. B.; Vermes, I.; Tibbe, A. G. J.; De Groot, M. R.; Terstappen, L. W. M. M. Importance of circulating tumor cells in newly diagnosed colorectal cancer. *Int. J. Oncol.* **2015**, *46* (3), 1361–1368.
- (7) Rack, B.; Schindlbeck, C.; Juckstock, J.; Andergassen, U.; Hepp, P.; Zwingers, T.; Friedl, T. W. P.; Lorenz, R.; Tesch, H.; Fasching, P. A.; et al. Circulating Tumor Cells Predict Survival in Early Average-to-High Risk Breast Cancer Patients. *J. Natl. Cancer Inst.* **2014**, *106* (5), DOI: [10.1093/jnci/dju066](https://doi.org/10.1093/jnci/dju066).

(8) Danila, D. C.; Fleisher, M.; Scher, H. I. Circulating Tumor Cells as Biomarkers in Prostate Cancer. *Clin. Cancer Res.* **2011**, *17* (12), 3903–3912.

(9) Pantel, K.; Hayes, D. F. Disseminated breast tumour cells: biological and clinical meaning. *Nat. Rev. Clin Oncol* **2018**, *15* (3), 129–131.

(10) Wang, C.; Mu, Z. M.; Chervoneva, I.; Austin, L.; Ye, Z.; Rossi, G.; Palazzo, J. P.; Sun, C.; Abu-Khalaf, M.; Myers, R. E.; et al. Longitudinally collected CTCs and CTC-clusters and clinical outcomes of metastatic breast cancer. *Breast Cancer Res. Tr* **2017**, *161* (1), 83–94.

(11) Trapp, E.; Janni, W.; Schindlbeck, C.; Juckstock, J.; Andergassen, U.; de Gregorio, A.; Alunni-Fabbroni, M.; Tzschaschel, M.; Polasik, A.; Koch, J. G.; et al. Presence of Circulating Tumor Cells in High-Risk Early Breast Cancer During Follow-Up and Prognosis. *Jnci-J. Natl. Cancer I* **2019**, *111* (4), 380–387.

(12) Dive, C.; Brady, G. SnapShot: Circulating Tumor Cells. *Cell* **2017**, *168* (4), 742.

(13) Yang, Y. P.; Giret, T. M.; Cote, R. J. Circulating Tumor Cells from Enumeration to Analysis: Current Challenges and Future Opportunities. *Cancers* **2021**, *13* (11), 2723.

(14) Loh, J.; Jovanovic, L.; Lehman, M.; Capp, A.; Pryor, D.; Harris, M.; Nelson, C.; Martin, J. Circulating tumor cell detection in high-risk non-metastatic prostate cancer. *J. Cancer Res. Clin* **2014**, *140* (12), 2157–2162.

(15) Cheng, Y. H.; Chen, Y. C.; Lin, E.; Brien, R.; Jung, S.; Chen, Y. T.; Lee, W.; Hao, Z. J.; Sahoo, S.; Kang, H. M.; et al. Hydro-Seq enables contamination-free high-throughput single-cell RNA-sequencing for circulating tumor cells. *Nat. Commun.* **2019**, *10*, 2163.

(16) Stott, S. L.; Hsu, C. H.; Tsukrov, D. I.; Yu, M.; Miyamoto, D. T.; Waltman, B. A.; Rothenberg, S. M.; Shah, A. M.; Smas, M. E.; Korir, G. K.; et al. Isolation of circulating tumor cells using a microvortex-generating herringbone-chip. *P Natl. Acad. Sci. USA* **2010**, *107* (43), 18392–18397.

(17) Yan, S. Q.; Chen, P.; Zeng, X. M.; Zhang, X.; Li, Y. W.; Xia, Y.; Wang, J.; Dai, X. F.; Feng, X. J.; Du, W.; et al. Integrated Multifunctional Electrochemistry Microchip for Highly Efficient Capture, Release, Lysis, and Analysis of Circulating Tumor Cells. *Anal. Chem.* **2017**, *89* (22), 12039–12044.

(18) Feng, J. M.; Mo, J. S.; Zhang, A. H.; Liu, D.; Zhou, L. F.; Hang, T.; Yang, C.; Wu, Q. N.; Xia, D. H.; Wen, R.; et al. Antibody-free isolation and regulation of adherent cancer cells via hybrid branched microtube-sandwiched hydrodynamic system. *Nanoscale* **2020**, *12* (8), 5103–5113.

(19) Zhu, S.; Jiang, F. T.; Han, Y.; Xiang, N.; Ni, Z. H. Microfluidics for label-free sorting of rare circulating tumor cells. *Analyst* **2020**, *145* (22), 7103–7124.

(20) Lee, S. J.; Lee, C. H.; Choi, S. H.; Ahn, S. H.; Son, B. H.; Lee, J. W.; Yu, J. H.; Kwon, N. J.; Lee, W. C.; Yang, K. S.; et al. Evaluation of a novel approach to circulating tumor cell isolation for cancer gene panel analysis in patients with breast cancer. *Oncol Lett.* **2017**, *13* (5), 3025–3031.

(21) Liu, Y. P.; Xu, H.; Li, T. Y.; Wang, W. Microtechnology-enabled filtration-based liquid biopsy: challenges and practical considerations. *Lab Chip* **2021**, *21* (6), 994–1015.

(22) Hao, S. J.; Wan, Y.; Xia, Y. Q.; Zou, X.; Zheng, S. Y. Size-based separation methods of circulating tumor cells. *Adv. Drug Deliver Rev.* **2018**, *125*, 3–20.

(23) Zhou, M. D.; Hao, S. J.; Williams, A. J.; Lv, B.; Zhu, J. Y.; Cote, R. J.; Datar, R. H.; Tai, Y. C.; Zheng, S. Y. Separable bilayer microfiltration device for viable label-free enrichment of circulating tumour cells. *Sci. Rep* **2014**, *4*, 7392.

(24) Bu, J.; Kang, Y. T.; Lee, Y. S.; Kim, J.; Cho, Y. H.; Moon, B. I. Lab on a fabric: Mass producible and low-cost fabric filters for the high throughput viable isolation of circulating tumor cells. *Biosens Bioelectron* **2017**, *91*, 747–755.

(25) Kim, T. H.; Lim, M.; Park, J.; Oh, J. M.; Kim, H.; Jeong, H.; Lee, S. J.; Park, H. C.; Jung, S.; Kim, B. C.; et al. FAST: Size-Selective, Clog-

Free Isolation of Rare Cancer Cells from Whole Blood at a Liquid-Liquid Interface. *Anal. Chem.* **2017**, *89* (2), 1155–1162.

(26) Nagrath, S.; Sequist, L. V.; Maheswaran, S.; Bell, D. W.; Irimia, D.; Ulkus, L.; Smith, M. R.; Kwak, E. L.; Digumarthy, S.; Muzikansky, A.; et al. Isolation of rare circulating tumour cells in cancer patients by microchip technology. *Nature* **2007**, *450* (7173), 1235–U1210.

(27) Gulati, G.; Song, J. M.; Florea, A. D.; Gong, J. Purpose and Criteria for Blood Smear Scan, Blood Smear Examination, and Blood Smear Review. *Ann. Lab Med.* **2013**, *33* (1), 1–7.

(28) Adewoyin, A. S.; Nwogoh, B. Peripheral blood film - a review. *Ann. Ib Postgrad. Med.* **2014**, *12* (2), 71–79.

(29) Melillo, A. Rabbit clinical pathology. *J. Exot Pet Med.* **2007**, *16* (3), 135–145.